Effects of Motility and Adsorption Rate Coefficient on Transport of Bacteria through Saturated Porous Media

Anne K. Camper, Jason T. Hayes, Paul J. Sturman, Warren L. Jones and Alfred B. Cunningham

***Appl. Environ. Microbiol.* 1993, 59(10):3455.**

APPLIED AND ENVIRONMENTAL MICROBIOLOGY, Oct. 1993, p. 3455–3462
0099-2240/93/103455-08$02.00/0

Vol. 59, No. 10

Effects of Motility and Adsorption Rate Coefficient on Transport of Bacteria through Saturated Porous Media

ANNE K. CAMPER,* JASON T. HAYES, PAUL J. STURMAN, WARREN L. JONES, AND ALFRED B. CUNNINGHAM

Center for Interfacial Microbial Process Engineering, Montana State University, Bozeman, Montana 59717

Received 8 March 1993/Accepted 21 July 1993

Three strains of *Pseudomonas fluorescens* with different motility rates and adsorption rate coefficients were injected into porous-medium reactors packed with 1-mm-diameter glass spheres. Cell breakthrough, time to peak concentration, tailing, and cell recovery were measured at three interstitial pore velocities (higher than, lower than, and much lower than the maximal bacterial motility rate). All experiments were done with distilled water to reduce the effects of growth and chemotaxis. Contrary to expectations, motility did not result in either early breakthrough or early time to peak concentration at flow velocities below the motility rate. Bacterial size exclusion effects were shown to affect breakthrough curve shape at the very low flow velocity, but no such effect was seen at the higher flow velocity. The tendency of bacteria to adsorb to porous-medium surfaces, as measured by adsorption rate coefficients, profoundly influenced transport characteristics. Cell recoveries were shown to be correlated with the ratio of advective to adsorptive transport in the reactors. Adsorption rate coefficients were found to be better predictors of microbial transport phenomena than individual characteristics, such as size, motility, or porous-medium hydrodynamics.

Schemes for enhancing in situ bioremediation of soil and groundwater generally involve injection and/or infiltration of fluid, nutrients, and oxygen (or other electron acceptors) to stimulate the growth of native microbial populations in the subsurface. In addition, suspension cultures of contaminant-degrading organisms may be added to the process stream to increase the amount of attached and suspended biomass within subsurface porous media. In the oil industry, the injection of starved microorganisms, or ultramicrobacteria (diameter, <0.3 μm), is a component of microbially enhanced oil recovery (13). These microorganisms are injected into an oil-bearing formation, transported to zones of high permeability, and then resuscitated. Growth of the bacteria resumes, and biofilms that selectively plug thief zones in the formation are formed. Vegetative bacteria have also been used in this manner. Although the success of these schemes depends upon site-specific microbial activity, little is currently known concerning the quantitative aspects of the transport, accumulation, and fate of the injected microorganisms. Consequently, the rational design and operation of microbial injection and/or infiltration systems are difficult.

In general, bacteria are chosen for bioremediation or microbially enhanced oil recovery on the basis of desired metabolic activities and/or products. However, other physiological characteristics, such as cell size (starved versus vegetative bacteria), motility, and cell surface properties (such as charge and hydrophobicity), may influence their transport through porous media and should be considered in the design of a delivery system.

The effects of motility on transport have been shown to be important in nonflowing systems in which chemotaxis is present (10). Reynolds et al. (18) found that motile strains of *Escherichia coli* penetrated four times faster than nonmotile mutants through nutrient-saturated sand-packed cores under static conditions. In contrast, in porous-medium reactors with no chemical gradients, the presence of flagella was not correlated with transport (1, 7).

Starvation or reduction in cell size may also affect bacterial transport by reducing the effects of filtration. In the absence of filtration, a smaller bacterium may have a reduced level of interaction with the porous medium along a pore channel and therefore may be more effectively transported. For example, MacLeod et al. (15) determined that starved *Klebsiella pneumoniae* cells penetrated farther through sintered glass bead columns and were distributed more evenly along the flow path than vegetative cells, even though the pores were considerably larger than the vegetative bacteria. This phenomenon was also observed with the same starved bacterium injected into 400-milliDarcy sandstone cores (13).

Cell hydrophobicity also has been investigated in relation to the ability of microorganisms to penetrate porous-medium columns. The transport of highly hydrophobic bacteria may be hindered or retarded by their tendency to adhere to porous media. Research by Gannon et al. (7) and Alexander et al. (1), however, showed no correlation between hydrophobicity and bacterial transport in soil columns. In addition, it was found that there was no relationship between capsule or polymer production and transport (7) in porous media. This result is in contrast to observations made with other systems; e.g., Mueller et al. (17) found a correlation between hydrophobicity and sticking efficiency for two *Pseudomonas* species, and Vanhaeke et al. (21) demonstrated a weak correlation between hydrophobicity and the propensity of *Pseudomonas aeruginosa* strains to adhere to stainless steel.

Cell surface charge may likewise influence the retention of bacteria in porous media. For example, Gannon et al. (7) and Alexander et al. (1) stated that surface charge, as measured by zeta potential, did not correlate with transport. However, in experiments in which fluids of increasing ionic strength were used, higher ionic strengths resulted in decreased bacterial transport (6, 8). It was hypothesized that increased

* Corresponding author.

ionic strengths decreased the thickness of the double layer on the surface and enhanced bacterial adsorption. Sharma et al. (19) stated that there was an excellent correlation between surface charge alteration and facilitated transport of two bacterial species through porous media.

The above-mentioned contradictory information on the relative importance of various cell characteristics in bacterial adsorption to and penetration through porous media prompted the approach for our research. Past work done in our laboratories has shown that the adsorption rate coefficient is a useful measure of the tendency for bacteria to adsorb to a surface. As defined by Mueller (16), the adsorption rate coefficient is a quantitative measure of the rate of movement of bacteria from the bulk fluid to the substratum (in this case, porous media) and the subsequent sticking of the bacteria to the surface. The transport component is affected by system hydrodynamics (flow regimen and velocity) and the diffusivity of the particles. Diffusivity of bacteria is governed by cell properties such as size and motility; small, motile bacteria exhibit greater diffusivity than large, nonmotile bacteria. Once a bacterium is transported to the surface, its ability to associate with the substratum relies on a variety of cell and substratum characteristics, such as bacterial hydrophobicity, bacterium-substratum charge interactions, surface roughness, and surface free energy. These interactions are described in an article by Loosdrecht et al. (14). Because transport and sticking efficiencies are combined in the adsorption rate coefficient, it may correlate better with bacterial movement through porous media than individual bacterial properties, such as size, motility, hydrophobicity, capsule production, and zeta potential. Experiments were devised with columns containing glass beads to examine the effects on bacterial transport of pore velocity, the bacterial adsorption rate coefficient, bacterial motility in the absence of chemotaxis, and cell size in the absence of filtration. The organisms tested included a motile *Pseudomonas fluorescens* strain, the same bacterium after starvation or size reduction, and a transposon mutant (Mot^-) of the same bacterium. Pulse injections of each bacterial type were passed through the porous-medium reactor at three pore velocities (125, 28, and 5.7 $\mu m\ s^{-1}$). These velocities correspond to calculated groundwater movements through medium-grain sand at gradients of 0.90, 0.18, and 0.032, respectively. Suspended-cell breakthrough curves were determined, and numbers of adsorbed bacteria inside the reactor were measured, thereby allowing cell mass balances to be computed.

MATERIALS AND METHODS

Reactor inocula. *P. fluorescens* CC-840406-E (Mot^+) and a nonmotile transposon mutant (Mot^-) were provided by Darren Korber, University of Saskatoon, Saskatoon, Saskatchewan, Canada. The bacteria were grown for 48 h at 35°C in 250-ml Erlenmeyer flasks containing 100 ml of mineral salts medium [0.7 g of K_2HPO_4, 0.3 g of KH_2PO_4, 0.1 g of $(NH_4)_2SO_4$, and 0.1 g of $MgSO_4 \cdot 7H_2O$ per liter] with 100 mg of glucose $liter^{-1}$. Stationary-phase bacteria were harvested by centrifugation at 4,000 × *g* for 10 min, washed once in sterile distilled water to remove traces of medium, and resuspended in 5 ml of sterile distilled water. Starved cells were prepared as described above but were resuspended in 100 ml of sterile mineral salts medium containing no glucose for 1 week. On days 1, 4, and 7 of starvation, cell size was determined by use of an image analysis system (American Innovision Videometric 150 software, version 4.33, and an Olympus BH-2 microscope).

Bacterial enumeration procedures. All enumerations (the reactor inoculum, each reactor effluent fraction, and all additional samples) were done in triplicate by the spread plate technique with R2A agar (Difco). Incubation was done for 48 h at room temperature. Reported values are the arithmetic means of the three appropriate plate counts.

Cell adsorption and size studies. Comparative levels of adherence of morphologically different *P. fluorescens* strains to either glass or polycarbonate surfaces were determined. The experimental system used was described by Escher (4). The motile and nonmotile bacteria were grown in a chemostat with a phosphate-buffered glucose solution (40 mg of glucose $liter^{-1}$; C/N ratio, <5) and a dilution rate of 0.2 h^{-1}; the yield was ca. 10^7 CFU ml^{-1}. Starved cells were prepared by centrifuging a chemostat culture of motile bacteria, resuspending the organisms in phosphate buffer, and keeping the culture at room temperature in a closed vessel for 7 days. The chemostat effluent and starved-cell culture were diluted 10-fold with phosphate buffer without glucose before entry into the flow cell to reduce the cell concentration to ca. 5.0 × 10^6 CFU ml^{-1}. A fluid shear stress of 0.75 N m^{-2} was used. Transmitted light and the image analysis system were used to visualize the number of bacteria that attached to and maintained contact with a known surface area of the glass or polycarbonate surface. Image frames were saved at regular intervals, and bacterial numbers, sizes, and locations were noted. By comparison of sequential frames, the number of cells per unit area per unit time was determined.

Using the method of Mueller (16), we calculated an adsorption rate coefficient. The overall adsorption rate was determined on the basis of bacterial cells per unit area per unit time (cells $mm^{-2}\ s^{-1}$). The number density of bulk fluid cells was measured (cells mm^{-3}). The adsorption rate coefficient is the overall adsorption rate divided by the cell concentration, or

$$\text{adsorption rate coefficient}\left(\frac{\text{meters}}{\text{s}}\right) = \frac{\text{overall adsorption rate (cells m}^{-2}\text{ s}^{-1})}{\text{bulk fluid cells (cells m}^{-3})} \quad (1)$$

It is important to note that the adsorption rate coefficient obtained by this method is specific for the experimental conditions and organisms for which it is determined.

Estimation of cell motility. For estimation of motility rates for the motile and starved motile bacteria, the glass surface in the flow cell was exposed to a bacterial suspension delivered at a shear stress of 0.75 N m^{-2} until a cell surface density of approximately 4.0 × 10^3 CFU mm^{-2} was reached (ca. 1 to 2 h). After initial adsorption occurred, the flow over the surface was terminated. Within 5 to 10 min, most of the initially adsorbed cells became motile and left the surface. The surface was monitored continuously at a magnification of ×1,500 and recorded on video tape by use of a high-resolution videocassette recorder. A television screen was calibrated by recording a microscope calibration slide at the same magnifications in horizontal and vertical directions. After the tape was replayed several times, the random free runs could be measured by marking the traveling phase (free run) and the twiddling phase (change in traveling direction). When the tape was replayed in slow motion with time control, the cellular swimming speed for a free run could be

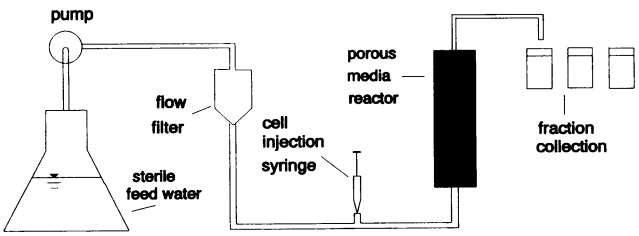

FIG. 1. Schematic diagram of the porous-medium reactor used to assess bacterial transport.

estimated from observations (16). The same procedure was used to verify that the Mot$^-$ bacteria were genetically stable and that no reversion mutations had occurred.

Porous-medium reactors. The basic reactor configuration is shown in Fig. 1. Glass beads (1 mm in diameter) that had been heated to 550°C for 4 h and cooled were added to polycarbonate tubes while the tubes were tapped. This method yielded a reproducible porosity of 0.38. The beads were kept in place with Teflon mesh on the inside of two rubber stoppers. The entire reactor was autoclaved at 121°C for 25 min. Sterile distilled water (ionic strength, <0.1 mM) was used as the influent medium after we determined that it did not affect the numbers of suspended bacteria during the time course of the experiments. The water was pumped from an Erlenmeyer flask into a flow filter that acted as a reservoir to dampen pulsing from the peristaltic feed pump. A short inoculum-dye injection port was located 10 cm upstream from the columns. The columns were operated in an upward-flow mode to minimize the effects of gravity, especially at the extremely low flow rates used.

Three reactors were designed to yield interstitial pore velocities that were higher than (125 $\mu m\ s^{-1}$), lower than (28 $\mu m\ s^{-1}$), and much lower than (5.7 $\mu m\ s^{-1}$) the maximal motility rates for the organisms tested (motile, 85 $\mu m\ s^{-1}$ [12], and starved motile, 150 ± 50 $\mu m\ s^{-1}$). Reactors 1 and 2 had a calculated residence time of approximately 50 min to minimize the possibility of cell replication in the reactors. No practical reactor design could be found to limit the residence time in reactor 3 with such a low flow rate; the calculated residence time was 292 min. This residence time corresponds to a dilution rate of 0.21 h^{-1}. Reactors 1 and 2 were fed with a Masterflex peristaltic pump (Cole-Parmer) with a size 14 pump head and tubing. Reactor 3 required the use of a Valleylab Infutrol 6000 infusion pump. Fluorescein dye tracer tests were run for each reactor to determine experimental residence times. The initial dye concentration was adjusted to an A_{488} of ca. 800 as measured with a Varian DMS90 spectrophotometer. A pulse dose of dye was injected, and the absorbances of successive fractions were measured. An experimental residence time was determined to be the time at which maximal dye recovery was obtained.

Penetrability studies. After the feed water was allowed to run through the reactor for a few minutes to fill the pore space, 2.5 ml of cell inoculum containing ca. 3.0×10^7 CFU ml^{-1} was injected by use of a sterile plastic syringe. Timing commenced at this point. At predetermined intervals, the cumulative reactor effluent for that period was collected in a sterile tube and the bacteria were enumerated. Time intervals for the two higher-flow reactors were 5 min for the first 1.5 h and 10 min for the remainder of the experiment. Effluent from the slow-flow reactor was collected at 15-min intervals.

Assays were performed to ascertain that motile bacteria had not lost their flagella during transport. One drop of a bacterial suspension obtained from the highest-flow reactor was placed on an oil-coated microscope slide, covered with a coverslip, and observed at ×100. Bacterial motility did not appear to differ between these organisms and those used to inoculate the tubes.

At the end of the low-flow experiments, a mass balance was performed to account for the injected cells. The water remaining in the reactor was drained, and the bacteria were enumerated. The glass beads were collected in a sterile 600-ml beaker. Sterile distilled water (180 ml) was added, and the beads were gently stirred with a glass rod to remove the loosely adherent cells. A sample of this fluid was homogenized, and the cell number was determined. The number of bacteria firmly adsorbed to the surface of the beads was determined by adding 5 ml of sterile distilled water and 0.01 ml of blending solution (2) to a ca. 25-g sample (22,000 beads) in a small beaker. The beads were sonicated in an ice bath for 30 s. A sample of the fluid was removed, and the bacteria were enumerated. After sonication, the bacteria remaining on the beads were fixed in 2% formaldehyde and stained overnight under refrigeration with acridine orange. After being rinsed, 5 to 10 beads were examined by epifluorescence microscopy and the number of bacteria per bead was recorded. In addition, the 10-cm hose section between the injection port and the reactor was removed and cut open, and the attached cells were scraped and enumerated by plate counting.

Each experiment was repeated at least twice under identical conditions. All penetrability results are plotted as C/C_o versus time, where C/C_o is the total number of cells in a sample divided by the total number of cells in the inoculum. The data reported are average results for these runs. The times at which initial breakthroughs and peak concentrations occurred varied slightly between experiments; true time averages could not be used, since samples were collected only at discrete time intervals. Therefore, the times at which initial and peak breakthroughs occurred in the individual replicate experiments were compared, and the one experimental time at which the highest cell number occurred was chosen to represent the average. Cell recovery data were obtained by determining the total number of effluent bacteria at each time, summing over the entire data collection period, and dividing the sum by the total number of bacteria injected into the reactor.

RESULTS

Motility study. The average motility for the starved bacteria was 150 ± 50 $\mu m\ s^{-1}$, determined as the mean of 47 observations. The average random free run was 33 ± 11 μm. No motility was noted in more than 100 observations for the nonmotile mutant.

Bacterial adsorption and size studies. Motile, nonmotile, and starved cells were examined for their propensity to adsorb to either glass or polycarbonate surfaces. These three cell types were to be used in the porous-medium experiments, and knowledge of their ability to adsorb to different reactor materials was desired. All three types of bacteria had slightly higher adsorption rate coefficients for glass than for polycarbonate. Starved cells had the highest adsorption rate coefficients (2.8×10^{-7} m s^{-1} on glass and 1.9×10^{-7} m s^{-1} on polycarbonate); motile cells were next (6.5×10^{-8} m s^{-1} on glass and 6.3×10^{-8} m s^{-1} on polycarbonate). Nonmotile

TABLE 1. Reactor specifications

Reactor	Volumetric flow rate (ml/min)	Tube dimensions (length × diam, cm)	Avg pore velocity (μm/s)	Hydraulic residence time (min)	
				Calculated	Actual
1	2.5	37.7 × 3.5	125	50	41
2	2.5	10 × 7	28	50	55
3	0.5	10 × 7	5.7	240	180

cells had the lowest adsorption rate coefficients (2.0×10^{-8} m s^{-1} on glass and 1.8×10^{-8} m s^{-1} on polycarbonate).

As determined by image analysis, healthy motile and nonmotile *P. fluorescens* cells had an average size of 1.5 by 0.5 μm. The starved bacteria were reduced in volume by ca. 25% within 7 days. Most of the size reduction was a result of shortening in length or "rounding" of the cells.

Reactor performance. Reactor specifications, operating conditions, and performance as determined by dye tracer studies are given in Table 1. For one reactor (reactor 2), the experimental residence time exceeded the calculated value by 10%. For the other two reactors, the experimental residence times were shorter than expected (82% of the calculated value for reactor 1 and 75% for reactor 3). All reactor flow velocities were within the laminar region (Reynolds number < 1).

Bacterial penetrability studies. The purpose of the penetrability studies was to determine how cell motility and adsorption affected the breakthrough of the bacteria under different flow rates in the absence of bacterial replication or chemotaxis. Reactor 1 was designed to produce an interstitial pore velocity higher than the maximal rate of motility for *P. fluorescens* (85 μm s^{-1} [12]). Although there were slight differences, all bacteria had similar average breakthrough curves (Fig. 2). Tailing occurred at very similar rates. The bacteria appeared to lag behind the dye in initial breakthrough and peak concentration (Table 2), but the maximum difference (ca. 0.2 pore volume) was only slightly higher than the error introduced by the 5-min sampling intervals (5 min divided by the 41-min residence time equals 0.12 pore volume). The average levels of cell recovery, which are indicative of the total numbers of injected bacteria that exited the reactor, were similar for the motile and nonmotile bacteria (Table 2). The level of recovery of the starved bacteria was much lower.

Reactor 2 was designed so that an interstitial pore velocity (28 μm s^{-1}) lower than the maximal rate of motility for *P. fluorescens* could be attained while maintaining a residence time similar to that in reactor 1. Average transport curves are shown in Fig. 3. The curves for all particles exhibited more tailing than that seen under the flow conditions in reactor 1; all cell types continued to be found in the effluent after the passage of 2.0 pore volumes. The starved motile cells showed the most tailing, while both the healthy motile and nonmotile cells had similar curve shapes. When sampling time error (5 min divided by 55 min equals 0.09 pore volume) was considered, the breakthrough of all bacteria preceded that of the dye (Table 2). This result was most pronounced with the motile bacteria. The starved cells were the first to reach peak concentration. The peak times for the motile and nonmotile bacteria were similar within the sampling time error. The starved bacteria had the lowest average cell recovery, while the motile and nonmotile bacterial cell recoveries were higher.

Average data from reactor 3 (pore velocity, 5.7 μm s^{-1})

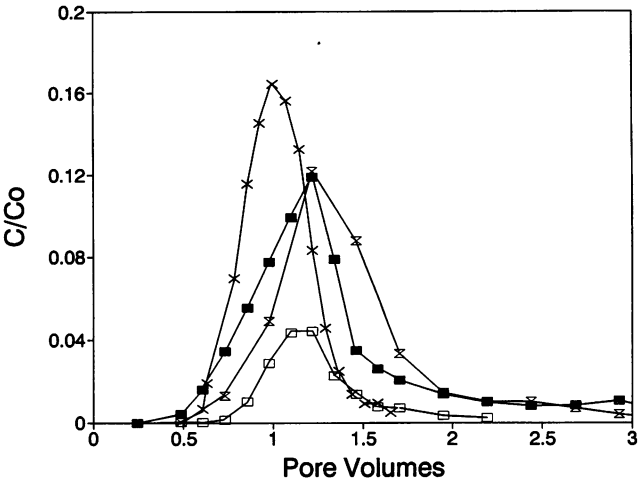

FIG. 2. Breakthrough curves for three bacterial types at an interstitial pore velocity of 125 μm s^{-1}. Each point is the arithmetic mean for two experiments. Ordinate values are the ratio of the number of bacteria enumerated during a sampling interval to the total number of injected bacteria. Pore volumes were calculated by use of the experimental residence time. Symbols: ×, dye; □, starved motile bacteria; ⧖, motile bacteria; ■, nonmotile bacteria.

are shown in Fig. 4. There was considerably more tailing with all three bacterial types as well as with the dye than at the other two flow rates. The starved cells ceased to exit the reactor after 1.15 pore volumes, and there were few motile bacteria in the reactor effluent after 2.5 pore volumes. A considerable number of nonmotile bacteria were enumerated in the effluent after 3.0 pore volumes. Another striking difference was the considerably larger area under the nonmotile bacterial curve compared with those for the two types of motile bacteria. These differences are reflected in the cell recoveries (Table 2), with starved-cell recovery being considerably lower than those for the two types of vegetative bacteria. The recovery of the nonmotile bacteria at this low flow rate was similar to that observed at the highest flow rate. Initial breakthrough of healthy motile cells and starved bacteria occurred at about 0.50 pore volume, while nonmotile cells first appeared at 0.30 pore volume. This initial breakthrough was the earliest observed for all bacteria and flow rates tested. These values indicate that, within error (0.08 pore volume), all bacterial types appeared in the reactor effluent in advance of the dye. When error was considered, the peak concentration for the two types of motile bacteria was reached before that for the dye (by 0.1 pore volume), while the nonmotile bacteria lagged behind the dye by the same amount.

Because of the low level of recovery of bacteria in the reactor effluent, a cell balance analysis of the contents of reactor 3 was performed at the end of the starved-cell experiments. Beads from the reactor were stained and examined for retained bacteria. Bacterial distribution was patchy, and approximately 10 bacteria per bead were counted. When this result was extrapolated to the entire reactor contents, we concluded that there was 10% retention on the beads. Including these organisms with those enumerated in the remainder of the reactor and those enumerated in the reactor effluent during the experiments (cell recovery data), we could account for an average of 11% of the starved bacteria, 55% of the motile bacteria, and 59% of the nonmotile bacteria injected into the reactor.

TABLE 2. Experimental values and means for initial breakthrough, peak bacterial concentration, and cell recovery for three bacterial types at three interstitial pore velocities

Bacteria	Values[a] in the indicated reactor[b] for:								
	Breakthrough[c]			Peak concn[d]			Cell recovery[e]		
	1	2	3	1	2	3	1	2	3
Starved	0.61, 0.61	0.45, 0.50	0.67, 0.58	1.22, 1.11	0.73, 0.64	0.83, 0.92	0.22, 0.17	0.23, 0.23	0.03, 0.02
Motile	0.49, 0.73	0.36, 0.45	0.5, 0.5	1.46, 1.22	1.10, 1.00	0.83, 0.83	0.29, 0.96	0.65, 0.39	0.25, 0.08
Nonmotile	0.49, 0.73	1.50, 0.45	0.33, 0.30	1.22, 1.22	0.910, 0.82	1.17, 1.17	0.82, 0.41	0.37, 0.26	0.17, 1.00
Means[f]									
Starved	0.61	0.50	0.58	1.22	0.73	0.83	0.20	0.23	0.03
Motile	0.49	0.36	0.50	1.22	1.10	0.83	0.63	0.42	0.17
Nonmotile	0.49	0.45	0.30	1.22	0.91	1.17	0.63	0.32	0.59
Dye	0.60	0.64	0.75	1.00	1.00	1.00	1.00	1.00	1.00

[a] Experiments were repeated twice.
[b] Reactor 1 interstitial pore velocity, 125 μm s^{-1}. Reactor 2 interstitial pore velocity, 28 μm s^{-1}. Reactor 3 interstitial pore velocity, 5.7 μm s^{-1}.
[c] Pore volume at which initial breakthrough was observed.
[d] Pore volume at which peak bacterial concentration was observed.
[e] Calculated as the number of bacteria in the total effluent volume divided by the total number injected.
[f] Calculated as described in Materials and Methods.

DISCUSSION

Conceptually, the transport of bacteria through porous media is dependent on (i) bacterial properties, such as size, motility, and surface hydrophobicity, (ii) porous-medium characteristics, such as porosity, tortuosity, particle diameter, and surface properties, and (iii) porous-medium hydrodynamics, including interstitial pore velocity and dispersivity. It is clear that a number of these characteristics, such as dispersivity, tortuosity, and pore water velocity, are interrelated. Furthermore, some characteristics interact synergistically to produce certain effects. A potentially important combination includes cell size, motility, cell surface hydrophobicity, porous-medium surface properties, and porous-medium hydrodynamics, since these affect the rate of transport and subsequent adsorption of cells to the porous-medium surface. As discussed above, the adsorption rate coefficient describes the net rate of adsorption and implicitly includes characteristics of the bacteria and hydrodynamics that affect adsorption. The following discussion will be oriented toward (i) effects of cell characteristics that would affect transport in the absence of sorption events and (ii) the effect of sorption on transport.

Motility and size effects. Nonchemotactic motility could affect bacterial transport by causing a portion of a motile population to emerge in advance of the tracer, especially at flow velocities lower than the average motility rate. Conversely, nonmotile bacteria may then behave as inert particles, be transported by advection and diffusion, and emerge with the fluid front. The effect of bacterial size, which has been shown to be important in transport (6, 7, 22), was tested with motile bacteria grown under nonlimiting conditions and starved motile bacteria. The effects of growth and chemo-

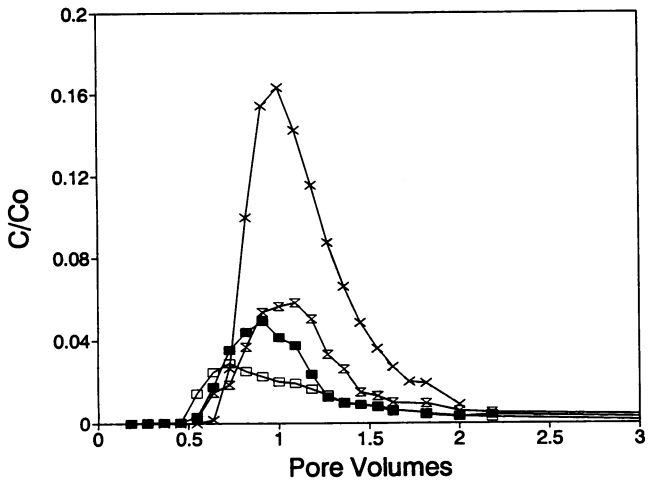

FIG. 3. Breakthrough curves for three bacterial types at an interstitial pore velocity of 28 μm s^{-1}. Each point is the arithmetic mean for two experiments. Ordinate values are the ratio of the number of bacteria enumerated during a sampling interval to the total number of injected bacteria. Pore volumes were calculated by use of the experimental residence time. Symbols are as defined in the legend to Fig. 2.

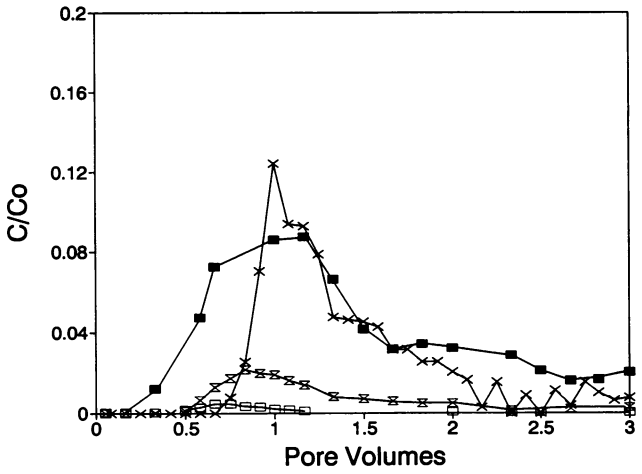

FIG. 4. Breakthrough curves for three bacterial types at an interstitial pore velocity of 5.7 μm s^{-1}. Each point is the arithmetic mean for two experiments. Ordinate values are the ratio of the number of bacteria enumerated during a sampling interval to the total number of injected bacteria. Pore volumes were calculated by use of the experimental residence time. Symbols are as defined in the legend to Fig. 2.

taxis, which have been shown to be important in bacterial movement through porous media (10, 18), were diminished in our experiments by the use of water with a very low carbon content and, when practical, reactor residence times that were shorter than the generation time of the bacteria.

The highest interstitial pore velocity used was higher than the maximal rate of motility for the Mot^+ bacteria. It was hypothesized that, under these conditions, the breakthrough curves for all cell types should resemble those obtained with the dye. All bacteria were transported at similar initial breakthrough and peak times. Fontes et al. (6) reported similar results in that cells of different sizes and analogous cell surface hydrophobicities behaved as particles and had similar retention times in both coarse- and fine-grained porous-medium reactors at a velocity of ca. 40 $\mu m\ s^{-1}$. In reactor 2, all three bacterial types appeared in the effluent in advance of the dye. The starved bacteria (the most motile and smallest) demonstrated an accelerated time to peak concentration. It should be noted, however, that this breakthrough curve was rather flat and the time to peak concentration was not clearly distinguishable. The most substantial differences in the temporal responses of the bacteria were seen at a pore velocity of 5.7 $\mu m\ s^{-1}$. The most pronounced change was seen in the behavior of the nonmotile bacteria, which showed the most tailing and by far the earliest breakthrough time.

In general, bacterial size and motility did not influence the time to peak concentration for the bacteria. This result has also been observed by others using a variety of porous media, especially under conditions of short transport distance (6, 9, 22).

Bacterial motility in the absence of chemotaxis could contribute to the initial appearance of cells in advance of the dye. It has been generally concluded, however, that motility is not important in the accelerated breakthrough of bacteria in porous media. For example, Harvey et al. (9) stated that motility was not a factor in the early bacterial breakthrough in their studies because of the short duration of their experiments and the lack of a chemical gradient. It is also probable that their bacteria, which had been stained with 4′,6-diamidino-2-phenylindole, were inactive and therefore nonmotile. In studies with 10 strains of flagellated bacteria in a column of sterile Kendaia loam and sterile water, transport was not related to motility (1, 7). Motility was not observed to produce early breakthrough in our experiments. At the lowest pore velocity, at which motility would be expected to make the most obvious contribution to early breakthrough, the nonmotile bacteria were the first to emerge.

The dispersion seen with the large, nonmotile bacteria is a phenomenon that has also been reported and explained by others. Fontes et al. (6), in laboratory experiments with quartz sand, reported that large bacteria were most affected by dispersion. Harvey et al. (9), in field studies with injected bacteria and a sandy aquifer, showed that inactivated bacteria appeared in distal recovery wells considerably in advance of the bromide tracer. These groups hypothesized that size exclusion, hydrodynamic chromatography, or phenomena related to distances between mixing points in the porous media contributed to the observations. These phenomena may also have contributed to the early nonmotile-cell breakthrough that we observed.

It was clear from our data as well as from those of others that the transport characteristics of bacteria cannot be predicted by use of size and motility information. Therefore, an alternative means of analyzing our data and a means of correlating bacterial attributes with transport were sought. The use of the adsorption rate coefficient, since it combines the influences of bacterial characteristics and hydrodynamics, was explored.

Effects of bacterial adsorption. In the preceding section, discussion centered on phenomena that were not related to adsorption and therefore ignored the variable recoveries and variable tailing phenomena in the breakthrough curves. The test strains were found to exhibit various adsorption rate coefficients. The starved bacteria, which had the highest motility rate, adsorbed most readily to glass and polycarbonate. The increase in the adsorption rate coefficient is consistent with reports that some bacteria exhibit enhanced "stickiness" after starvation (3, 11). It is important to note, however, that not all starved bacteria, or ultramicrobacteria, exhibit this characteristic. The lowest coefficient was calculated for the nonmotile bacteria; the value for the motile bacteria was intermediate. It was of interest to determine the manner in which adsorption to the porous media would affect the overall transport of the strains through the columns.

An important characteristic of bacterial transport in porous media is cell recovery, which is usually reported as the cumulative number of bacteria enumerated in reactor effluent aliquots in comparison with the injected number of bacteria. This value can be affected by a variety of factors, including filtration, adsorption, and cell death. In the presence of filtration, reported effluent recovery values are 0.01 to 15% in Kendaia loam (7), 0 to 25% in soil and aquifer sand (1), <1% for large bacteria in fine-grained columns with high-ionic-strength transport medium to 90% for small bacteria in coarse-grained columns with low-ionic-strength medium (6), and near 100% in aquifer sand with distilled water (8). In our experiments, which used distilled water to reduce ionic effects, average recovery values did not approach 100%. The highest level of recovery was obtained with the motile and nonmotile bacteria at the highest flow rate. The starved bacteria, which had the highest adsorption rate coefficient, exhibited an inverse relationship between recovery and pore velocity.

When analyses were performed at the end of the low-flow experiments to account for the remainder of the injected bacteria, the balance still could not be closed. Recovery was least improved with the low-adsorption-rate-coefficient nonmotile bacteria and most improved with the motile bacteria. Only a 6% increase in starved bacterial recovery was obtained. It was hypothesized that significant cell death must have been occurring, even though it was confirmed that suspension of the bacteria in distilled water did not decrease bacterial viability during the time courses of the experiments. This phenomenon was not explored by the majority of researchers, who presumed that the unaccounted bacteria were retained in the porous media (1, 6–8, 20). Only Wollum and Cassel (22) enumerated the number of organisms either filtered by or adsorbed to the porous media; their total bacterial recovery was 5.6%. If a threshold population of potentially active bacteria is required in a particular field application, any transport scheme developed to deliver those organisms should consider the possibility of substantial microbial loss even in the absence of predation.

Except for results obtained at the highest flow rate, at which all bacteria behaved as particles, substantial tailing, which was inversely related to flow rate, was observed with the bacteria. Significant tailing of bacteria and conidia in porous media with the potential for filtration has also been reported by others (6, 22). Fontes et al. (6) hypothesized that tailing is the result of the flushing of previously retained

bacteria. In our experiments, the tailing effect was most probably not related to the mobilization of filtered bacteria because of the overall large pore size in the porous media. It was more likely related to the detachment of loosely adsorbed bacteria. This hypothesis is supported by several observations. At the lowest pore velocity, the least amount of tailing was observed with the highly adsorptive, starved bacteria. The fluid shear stress (7.1×10^{-5} N m^{-2}) may have been insufficient to remove these bacteria. The motile bacteria, which had an intermediate adsorption rate coefficient, detached, resulting in significant tailing. The least adsorptive, nonmotile bacteria were easily sheared and appeared in the reactor effluent after 3.0 pore volumes. At the intermediate pore velocity, the most dramatic tailing was seen with the starved bacteria. The fluid shear stress (3.5×10^{-4} N m^{-2}) may have been sufficient to remove the motile and nonmotile bacteria; only the starved bacteria resisted desorption. At the highest pore velocity (and therefore the highest fluid shear stress 1.6×10^{-3} N m^{-2}), only irreversibly adsorbed bacteria of all types remained on the glass beads, and no tailing was produced. Further confirmation of these conclusions can be drawn from the strong negative correlation found between adsorption rate coefficient and increased shear stress by Escher and Characklis (5); fewer bacteria accumulated on a surface at higher fluid velocities.

Since it was apparent that bacterial adsorption was an important phenomenon in these experiments, a mathematical description for the relationship between adsorptive transport and advective transport of bacteria in porous media was developed. The relationship can be seen by comparing the flux of bacteria to the surface of the porous-medium particles with the overall flux through the system. The overall number of bacteria entering a section of the column per unit of time (the advection rate) may be expressed as

$$\text{advection}\left(\frac{\text{cells}}{\text{time}}\right) = QC = V_p \varepsilon A_x C \qquad (2)$$

where Q is the flow rate, V_p is the mean pore velocity (micrometers per second), ε is the porosity, A_x is the column cross-sectional area, and C is the bacterial concentration (cells per milliliter). In a similar fashion, the total number of bacteria adsorbing to the media per unit of time (the adsorption rate) within a column section in the system can be approximated by

$$\text{adsorption}\left(\frac{\text{cells}}{\text{time}}\right) = V_A A_p C \qquad (3)$$

where V_A is the adsorption rate coefficient and A_p is the surface area of porous-medium particles available for colonization. The area, A_p, can be expressed as the product of the specific surface area, a, and the total column volume, $A_x L$, where L is the column length. For a random packing of uniform spheres, it can be shown that a is given by

$$a = 6(1 - \varepsilon)/d_p \qquad (4)$$

Thus, a dimensionless flux ratio, J^*, can be obtained by dividing equation 2 by equation 3 to compare the advection rate with the adsorption rate:

$$J^* = (V_p/V_A)\{\varepsilon/[6(1 - \varepsilon)]\}(d_p/L) \qquad (5)$$

It should be noted that this ratio can also be viewed as a ratio of the time needed for adsorption $\{\varepsilon d_p/[6(1 - \varepsilon)V_A]\}$ to the residence time in the column (L/V_p). If the time required for adsorption greatly exceeds the residence time of the system, relatively little adsorption is expected. Conversely, if the time required for adsorption is short compared with the reactor residence time, significant retention of adsorbed bacteria is expected.

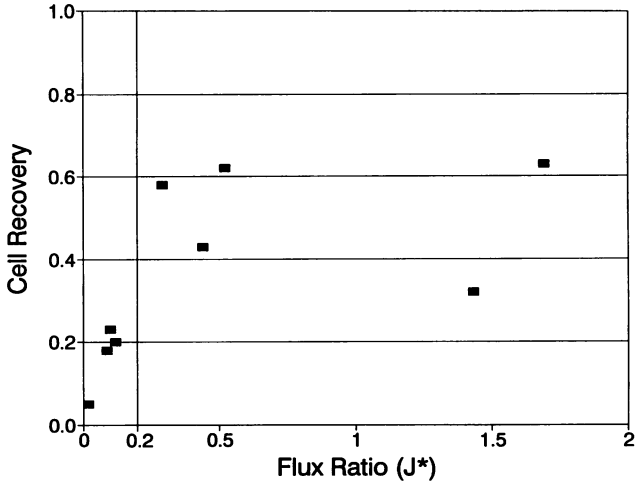

FIG. 5. Mean cell recovery (percent) plotted against the dimensionless flux ratio (J^*) calculated from equation 5.

The quantity J^* was determined for each of the combinations of bacterial adsorption velocities and pore velocities. The recovery of organisms from the various experiments is plotted against J^* in Fig. 5. Recoveries were low in experiments in which J^* was <0.2. When J^* exceeded 0.2, recoveries were still less than 100% but were notably higher than in the experiments in which J^* was <0.2. Some adsorption is always expected because of the tortuosity of the fluid path (increasing the convective transport of cells toward particle surfaces), local decreases in fluid velocity, and filtration effects. Thus, the recovery is never expected to reach 100%, even for high J^* values. From a practical standpoint, a direct measurement of adsorption rate coefficient on natural soil materials is nearly impossible. Nevertheless, it is interesting that the ratio of advection rate to adsorption rate (J^*) was qualitatively related to recovery over a wide range of pore velocities, motility rates, and cell sizes.

ACKNOWLEDGMENTS

We thank Marty Hamilton for assistance with our statistical presentation. We also thank Robert Mueller and Ross Lundman for lively discussions and helpful insights into adsorption and porous medium transport.

This work was supported by Cooperative Agreement ECD-8907039 between the National Science Foundation and Montana State University. Funding was also provided under agreement R-815709 to Montana State University through the Hazardous Substance Research Center for U.S. E.P.A. regions 7 and 8 at Kansas State University.

REFERENCES

1. **Alexander, M., R. J. Wagenet, P. C. Baveye, J. T. Gannon, U. Mingelgrin, and Y. Tan.** 1991. Movement of bacteria through soil and aquifer sand. Environmental Protection Agency project summary EPA/600/S2-91/010. Environmental Protection Agency, Washington, D.C.
2. **Camper, A. K., M. W. LeChevallier, S. C. Broadaway, and G. A. McFeters.** 1985. Evaluation of procedures to desorb

bacteria from granular activated carbon. J. Microbiol. Methods **3:**187–198.
3. **Dawson, M. P., B. Humphrey, and R. C. Marshall.** 1981. Adhesion: a tactic in the survival of a marine *Vibrio* during starvation. Curr. Microbiol. **6:**195–201.
4. **Escher, A. R.** 1986. Colonization of a smooth surface by *Pseudomonas aeruginosa*: image analysis methods. Ph.D. dissertation. Montana State University, Bozeman.
5. **Escher, A. R., and W. G. Characklis.** 1990. Modeling the initial events in biofilm accumulation, p. 445–486. *In* W. G. Characklis and K. C. Marshall (ed.), Biofilms. John Wiley & Sons, Inc., New York.
6. **Fontes, D. E., A. L. Mills, G. M. Hornberger, and J. S. Herman.** 1991. Physical and chemical factors influencing transport of microorganisms through porous media. Appl. Environ. Microbiol. **57:**2473–2481.
7. **Gannon, J. T., V. B. Manilal, and M. Alexander.** 1991. Relationship between cell surface properties and transport of bacteria through soil. Appl. Environ. Microbiol. **57:**190–193.
8. **Gannon, J. T., Y. Tan, P. Baveye, and M. Alexander.** 1991. Effect of sodium chloride on transport of bacteria in a saturated aquifer material. Appl. Environ. Microbiol. **57:**2497–2501.
9. **Harvey, R. W., L. H. George, R. L. Smith, and D. R. DeBlanc.** 1989. Transport of microspheres and indigenous bacteria through a sandy aquifer: results of natural- and forced-gradient tracer experiments. Environ. Sci. Technol. **23:**51–56.
10. **Jenneman, G. E., M. J. McInerney, and R. M. Knapp.** 1985. Microbial penetration through nutrient-saturated Berea sandstone. Appl. Environ. Microbiol. **50:**383–391.
11. **Kjelleburg, S., and M. Hermansson.** 1984. Starvation-induced effects on bacterial surface characteristics. Appl. Environ. Microbiol. **48:**497–503.
12. **Korber, D. R., J. R. Lawrence, B. Sutton, and D. E. Caldwell.** 1989. Effect of laminar flow velocity on the kinetics of surface recolonization by mot$^+$ and mot$^-$ *Pseudomonas fluorescens*. Microb. Ecol. **18:**1–19.
13. **Lappin-Scott, H. M., F. Cusack, and J. W. Costerton.** 1988. Nutrient resuscitation and growth of starved cells in sandstone cores: a novel approach to enhanced oil recovery. Appl. Environ. Microbiol. **54:**1373–1382.
14. **Loosdrecht, M. C. M., J. Lyklema, W. Norde, and A. Zehnder.** 1989. Bacterial adhesion: a physicochemical approach. Microb. Ecol. **17:**1–15.
15. **MacLeod, F. A., H. M. Lappin-Scott, and J. W. Costerton.** 1988. Plugging of a model rock system by using starved bacteria. Appl. Environ. Microbiol. **54:**1365–1372.
16. **Mueller, R. F.** 1990. Characterization of initial events of bacterial colonization at solid-water interfaces using image analysis. M.S. thesis. Montana State University, Bozeman.
17. **Mueller, R. F., W. G. Characklis, W. L. Jones, and J. T. Sears.** 1992. Characterization of initial events in bacterial surface colonization by two *Pseudomonas* species using image analysis. Biotechnol. Bioeng. **39:**1161–1170.
18. **Reynolds, P. J., P. Sharma, G. E. Jenneman, and M. J. McInerney.** 1989. Mechanisms of microbial movement in subsurface materials. Appl. Environ. Microbiol. **55:**2280–2286.
19. **Sharma, M. M., Y. I. Chang, and T. F. Yen.** 1985. Reversible and irreversible surface charge modifications of bacteria for facilitating transport through porous media. Colloids Surf. **16:** 193–206.
20. **Smith, M. S., G. W. Thomas, R. E. White, and D. Ritonga.** 1985. Transport of *Escherichia coli* through intact and disturbed soil columns. J. Environ. Qual. **14:**87–91.
21. **Vanhaeke, E., J. P. Remon, M. Moores, F. Raes, D. De Rudder, and A. Van Petighem.** 1990. Kinetics of *Pseudomonas aeruginosa* adhesion to 304 and 316-L stainless steel: role of cell surface hydrophobicity. Appl. Environ. Microbiol. **56:**788–795.
22. **Wollum, A. G., II, and D. K. Cassel.** 1978. Transport of microorganisms in sand columns. Soil Sci. Soc. Am. J. **42:**72–76.